JOURNAL OF CATALYSIS 140, 464–480 (1993)

AC Electrical Characterisation of Heterogeneous Catalysts

A. OVENSTON[1] AND J. R. WALLS*

*Chemical Engineering, School of Science & Technology, University of Teesside, Middlesbrough, Cleveland, TS1 3BA, United Kingdom; and *Department of Chemical Engineering, University of Bradford, Bradford, West Yorkshire, BD7 1DP, United Kingdom*

Received March 18, 1992; revised October 19, 1992

At operating temperatures, heterogeneous catalysts behave like lossy dielectrics. The technique of impedance spectroscopy has been used in conjunction with other AC methods to differentiate between different loss processes. At low frequencies and high temperatures, thermally activated hopping of relatively free charges is dominant, whilst at higher frequencies and lower temperatures relaxation losses from dipoles at the surface and in the bulk of the material prevail. The principal use of impedance spectroscopy is in the determination of geometry-independent parameters. These help to elucidate the roles of the insulating and conducting components in a catalyst and define the frequency and temperature ranges over which various processes predominate. In general, the dielectric–frequency relationships are in agreement with the models for the "universal" dielectric behaviour of solids. The electrical parameters are highly sensitive to inherent changes in catalysts and hence these AC methods offer potential *in-situ* techniques for studying factors such as chemisorption, deactivation, activity, selectivity, phase changes, and solid-state reactions.

INTRODUCTION

A study of the AC electrical properties of heterogeneous catalysts has arisen from the need to design ceramic composites of high loss for use as catalysts which can be heated by electromagnetic RF power (*1*, *2*). For materials without a ferromagnetic component the energy absorbed in a given electromagnetic field is proportional to the AC conductivity (σ_{AC}). At RF, this arises from the motion of relatively mobile charge carriers (electrons, ions, or complexes) and from dipole relaxation processes from charges which are more closely bound to the lattice. The conductivity of the composite largely depends on frequency and temperature (*3*, *4*), but it may also depend on atmosphere and time. Chemisorption has been shown to have a significant and rapid effect on the DC characteristics of supported Ni and Pt/TiO_2 catalysts (*5*, *6*) and on the AC characteristics of composites of higher conductivity (*7*). Longer time effects may be indicative of bulk rather than surface chemical changes, the occurrence of solid state reactions between components, or of sintering processes (*8*).

Materials for use in AC fields must be able to heat up rapidly and remain at reaction temperatures without significant thermal fluctuations or the possibility of thermal runaway (*1*, *2*, *9*). For this purpose conducting mixed oxides have been found to be satisfactory, such as alkali tungsten bronzes or potassium magnesium titanates, mixed with an insulating support in proportions approaching the percolation threshold. These materials, their preparation, and catalytic activity have been described in detail elsewhere (*4*, *10*).

If the conductivity is predominantly electronic, DC measurements using Pt electrodes are adequate. However, if in addition, diffusion of ions is present at reaction temperatures, a slow build-up of ions will

[1] To whom correspondence should be addressed. Present address: Department of Chemical Engineering, University of Bradford, Bradford BD7 1DP, U.K.

0021-9517/93 $5.00

occur at the electrodes and will distort the measurements. This limitation of electrode polarisation can be avoided by using AC techniques. The measured conductivity then represents the summation of all loss processes due to all types and varieties of charged species. AC conductance techniques can be used to separate electrode polarisation effects from the bulk conductance and allow a more detailed analysis of the various contributions to charge transport, as described in more detail in the next section.

Atkinson has recently drawn attention to the importance of grain boundary diffusion in ceramics (*11*, *12*). This may be faster or slower than bulk diffusion depending on the material and ions involved, with a variety of possible mechanisms for their diffusional transport. Point defects are associated with both lattice and grain boundary diffusion and impurities segregating to the boundary can have a considerable blocking effect; furthermore, interactions between point defects and impurities may occur. In the case of composite materials of high AC conductivity for use in RF reactors the control of AC loss processes and transport of charge carriers through the lattice or via grain boundaries or surfaces is particularly important. Impedance spectroscopy is an AC technique which was developed to study relatively simple single crystals or polycrystalline samples of ionic conductors. This paper discusses its potential use to separate the contributions to resistivity from the intrinsic nature of the material itself, the grain boundaries, and electrode polarisation effects (e.g., *13*, *14*). Previous research has shown that composite catalytic materials exhibit the "universal" dielectric type of behaviour which is characteristic of a large range of solid dielectric solids, as explored by Jonscher and Hill (*3*, *4*, *15–17*). There are consequently two schools of thought which may be applied to the interpretation of the complex impedance spectra of composite dielectric materials. This paper examines impedance data between 100 Hz and 10 MHz over temperatures between 300 and 1000 K for a variety of catalytic materials with a range of electrical properties. It is shown that the two approaches are not incompatible and indeed can be complementary. Considerable support for the Jonscher–Hill model is shown, whilst surface and bulk effects are best interpreted using the simpler models of impedance spectroscopists.

Such a knowledge of the dielectric behaviour of catalysts is important particularly to design materials to be used in electromagnetic fields and also to assist in the understanding of catalytic processes, some of which are known (e.g., oxidation catalysts) to be affected not just by charge transfer at the catalyst surface but also within the bulk of the materials.

Catalytic behavior is generally associated with the formation of dipole bonding through chemisorption and diffusion of charges at the exposed surfaces of the materials. Electrons and ions (often chalcogenide and oxygen anions) may be required to be supplied to this surface in order to maintain catalytic activity; thus the transport of charges from the bulk of the material to the surface and intercrystalline layers can play an important role. Materials containing both high electronic and/or ionic conductivity are considered necessary for reactions in which high bulk mobilities of the charges are required in addition to specific surface characteristics. For example, mixed conductors (having significant electronic and ionic conductivity) are required in selective oxidation catalysis (*18*). In catalysts having structures which facilitate diffusion of oxygen from surface oxygen chemisorption sites to subsurface vacancies, reoxidation proceeds rapidly. Transformation of oxygen to O^{2-} requires electron transfer from the solid in order to activate and dissociate the O_2 prior to incorporation into the vacancy.

In a recent review, Gellings and Bouwmeester (*19*) have concluded that the conducting properties of ion and mixed conducting oxides exert a great influence on

their catalytic behaviour. The diffusivity of oxygen vacancies is particularly important but the electronic contribution to the total conductivity also plays a significant role. They emphasise that further research is needed to understand better the correlations between catalytic properties and conduction properties. They also stress that there is an urgent need to study the relation between the conducting properties of the bulk and surface regions, which may differ due to space charge and/or segregation effects. Here, Impedance Spectroscopy could play an important role.

Pritchard (*20*) has also recently drawn attention to the fact that long range electronic interactions can be important, in addition to short range effects associated with specific surface sites. Work function changes reflecting long-range electronic effects have been successfully used to show a relationship with catalytic rate enhancements and activation energies for a wide range of reactions on various supported metal catalysts (*21*).

As in the case of making new ceramics, a rational synthesis of a catalyst generally depends on an understanding of the physics and chemistry of particulates; defects in materials which influence charge carrier mobilities can also strongly influence the catalytic properties and lifetimes of catalysts. Thomas (*22*) has highlighted the control of the catalytic peformance of perovskites (for which the simplest form is ABO_3 (*23*)) in which loss of oxygen is associated with the inherent oxygen anion vacancies. Those reactions difficult to catalyse such as the oxidative coupling of methane may come into this category (*24*). Carberry *et al.* (*25*) have recently reported the possible substitution of solid oxide solutions as a replacement for expensive supported Pt catalysts for CO oxidation in fume abatement, without reduction in activity on exposure to H_2S, and for the hydrogenation of propylene. These materials have the additional advantage that they are sintered during preparation and are consequently less subject to deactivation by sintering during use.

Muragaraj and Maier (*26*) in their work on the enhancement of ionic conductivity of solid electrolytes with the addition of a finely dispersed insulating phase (Liang effect) have shown that such composite electrolytes containing ionic defects can also act as effective heterogeneous catalysts. Effects from the variation in catalyst composition resembling the Liang effect have been shown in our own mixed oxide composites both at DC and AC (*1*). High electronic conductivity can also favour catalytic activity (*27*). There are many other examples of enhancement of activity from increased conductivity in the bulk of the material.

Thus the time is ripe for exploring the electrical properties of composite mixed oxides with or without insulating supports not just for their use in RF reactors, for which they are eminently suited, but also for studying their potential as catalysts for both new and well established reactions in more conventional reactors.

Equivalent Circuits

Multicomponent porous catalysts containing both insulating and conducting components behave like solid dielectrics which have high loss at high temperatures. For perfect dielectrics the current is 90° out of phase with the applied voltage and there is no power loss; however, lossy materials require that there is a component of current in phase with the voltage which is the cause of heating in an applied AC field (*28–30*).

Single parallel R–C circuit. Such dielectrics can be represented by a complex permittivity/dielectric constant ($\varepsilon' = \varepsilon' - i\varepsilon''$), where $i = \sqrt{(-1)}$ (*15, 31*). The material behaves like a perfect capacitance (C_p) with a parallel resistance (or conductance $G = R^{-1}$), where both $\varepsilon' \propto C_p$ and $\varepsilon'' \propto G/\omega$ vary with frequency (ω = angular frequency = $2\pi f$) and temperature (Fig. 1). The loss tangent, a parameter independent of geometry, given by $\tan \delta = \varepsilon''/\varepsilon'$, is often quoted and is useful for comparing the loss characteristics of different materials (*28*).

Dielectric dispersion curves in which log

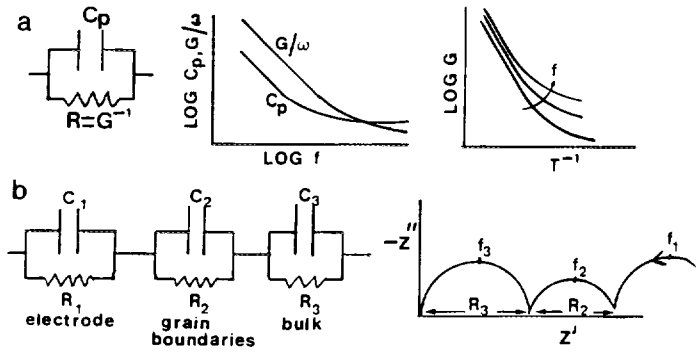

FIG. 1. Electrical representation of a catalyst. (a) Single parallel R–C circuit and (b) series of parallel R–C circuits, $f_i = (2\pi R_i C_i)^{-1}$. For symbols, see text.

ε' and log ε'' are plotted as functions of log frequency are commonly used to describe the dielectric behaviour. For a given material these curves often have the same shape at all temperatures, or other variables such as the degree of moisture (*3*) and may be normalised by displacement of the axes (e.g., Ref. *17*)). Earlier work has shown that both commercial supported Ni catalysts and those containing mixed or ionic conductors behave in this way, i.e., with the "universal" type of dielectric response characteristic of many dielectrics in which hopping charge carriers are present (at high temperatures) and give rise to an anomalous low-frequency dispersion (*3, 4*). Jonscher (*16,32*) has shown that this non-Debye type of behaviour can be described by real and imaginary components of susceptibility which are independent of frequency but related by a power n, $(0 \leq n < 1)$ such that

$$\chi''/\chi' = \cot(n\pi/2).$$

Now $\chi^*(\omega) = \varepsilon^*(\omega) - \varepsilon_\infty$, where ε_∞ is the limiting value of ε' at high frequencies. Thus at high temperatures, $\varepsilon'' \gg \varepsilon_\infty$ and $\tan\delta = \varepsilon''/\varepsilon' = \cot(n\pi/2)$.

At low frequencies/high temperatures n approaches zero and represents a "hopping" charge carrier effect resulting from screening due to "many-body" interactions, whilst at high frequencies/low temperatures n approaches values of about 0.7 and is a "lattice" response from a regular array of permanent or induced dipoles without screening effects. Thus by measurements of G and C_p as functions of frequency and temperature, the validity of the above relationships can be tested. Low values of n are accompanied by high activation energies of the order of 1 eV, typical of predominantly "free" charge behaviour; high values of n are accompanied by much reduced activation energies which may even approach zero if thermal activation plays a negligible role in determining the dielectric loss.

Series of parallel R–C circuits. For single component ionic conductors when the real and imaginary components of the impedance (resistance and reactance in series) are plotted on a complex plane diagram over a wide range of frequencies, a series of well defined semicircles can be identified with specific loss processes (Fig. 1) (*14*). In contrast to the single R–C circuit, each circuit is representative of an individual loss phenomenon (bulk, grain boundary or electrode); in each R–C unit the R and C values are independent of frequency and have a characteristic frequency $f_0 = (2\pi RC)^{-1}$ at which the process is dominant. Some materials are better represented by more complex circuits (see, for example, Ref. *33*)). Such a method of analysis is known as "Complex Impedance Spectroscopy" and may be tested by seeing how well such R–C

networks fit the data. In practice semicircles are often found, especially at higher frequencies, but may be tilted to the Z' axis, and at low frequencies straight line spurs may be observed.

There are few references to application of this technique to composite materials, although a solid electrolyte dispersed in alumina has been studied and this illustrated the effect of the proportions of the two components (*34*). Conducting additives make a significant contribution to dipole relaxation losses at RF and contain mobile electrons as well as ions (of one or more species) which may diffuse throughout the composite at high temperatures. In general, the complex impedance diagrams revealed a low frequency spur at high temperatures for materials containing fast ions and a semicircle at lower temperatures/higher frequencies for all the materials investigated. This paper examines the complex plane impedance plots and their accompanying dielectric dispersion curves for a variety of catalytic materials.

METHODS

Preparation of Composites

For the samples containing conducting mixed oxides, the components ($K_{0.5}WO_3$ and $K_xMg_yTi_{1-y}O_2$) were prepared by a fusion method which involves direct heating of oxides at 1273 K for 12 hours (*4*). The product is finely ground and wet mixed to form a stiff paste with a high-alumina cement and alumina or Portland cement (with 35 wt% of the conducting component, unless otherwise stated). The cement in the extruded pellets (1.5 mm diameter, 1 to 5 mm thick) is allowed to set over a water bath for 5 days. For experiments on the I.C.I. steam reforming silica–alumina-supported Ni catalyst (46-1) the cylindrical pellets were 15 mm diameter, 15 mm long, and contained a central hole. In the prereduced state, this catalyst typically contains NiO (21%), CaO (11%), SiO_2 (16%), Al_2O_3 (32%), MgO (13%) and K_2O (7% by wt). Electrical contacts were applied to the end faces of the samples using a Johnson Matthey Pt-based enamel (E-831) fired on at 973 K for 1 hr. For the Ni catalyst an Au enamel paste was also tested, but not used for other samples due to a tendency to flake-off with time.

Furnace

A Eurotherm gold reflecting furnace (106) with a controller/programmer unit (812) was used to control the temperature between 300 and 1000 K. The temperature was measured by a chromel–alumel thermocouple placed inside a vitreous silica high-temperature tube in the furnace near to the sample. The temperature was maintained at set values for at least 30 min or until the electrical parameters had become stable. Experiments were conducted in a stream of predried Ar at 100 ml/min except where stated otherwise. Effects of H_2 and CO_2 were determined by mixing with Ar (each gas flowing at 50 ml/min) using Brooks flowmeters and a control unit.

Electrical Measurements

A Hewlett–Packard programmable Impedance Analyser 4194A was used to determine the variation of electrical properties with temperature and frequency (100 Hz to 2.5 MHz). High-temperature BICC Pyrotenax shielded Cu leads with flat brass contacts were used to hold the sample under compression, these being connected to Hewlett–Packard test leads 16048A outside the furnace. The effect of the leads was deducted from the measurements using the compensation facility of the instrument.

The samples were represented by a resistance and capacitance in parallel for dielectric dispersion and loss tangent measurements and by a resistance and reactance in series for complex impedance measurements (see the preceding section on Equivalent Circuits). In some cases the complex admittance ($Y = 1/Z$) and complex electric modulus ($M^* = (\varepsilon^*)^{-1}$) were also measured.

Moisture is readily absorbed by catalytic materials which contain a fine pore structure. Hence, prior to any electrical studies

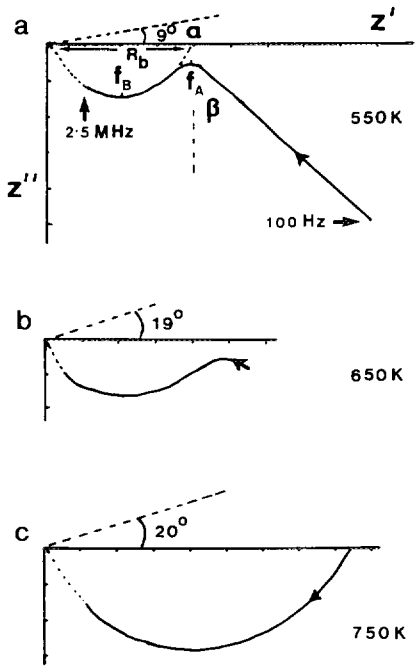

FIG. 2. Typical complex impedance plane diagrams for composites containing insulators plus (a) an ionic, (b) a mixed, and (c) an electronic conductor.

samples must be predried in an inert atmosphere at about 400 K until the electrical characteristics become stable and the moisture has been desorbed as far as possible. The effect of this drying-out process is easily detected by following the changes in the electrical data. When any electrical parameters were plotted as a function of frequency and time moisture was found to have the greatest effect at the lower frequencies.

RESULTS

Typical impedance plane diagrams for composites containing essentially (a) an ionic conductor ($K_{0.5}Mg_{0.8}Ti_{0.2}O_2$), (b) a mixed conductor ($K_{0.5}WO_3$) and (c) an electronic conductor (Ti_4O_7) mixed with an insulating support (in proportions near to but below the percolation threshold) are shown in Fig. 2. Since the reactance Z'' is essentially capacitative, Z'' is negative for all the data discussed. In much published work it is often represented by the positive quantity $|Z''|$.

For the predominantly ionic component, in which K^+ ions are able to move easily along one-dimensional channels in the hollandite structure (*4*), a well defined semicircle is observed at high frequencies and low temperatures with a small angle of tilt (about 9°) to the Z′ axis. This is typical of ionic electrolytes, e.g., yttria-stabilised zirconia (*35*). At low frequencies a spur becomes attached and is associated with the diffusion of relatively free ions; although it is apparently a straight line it could be an arc of a very large semicircle. Angles of 45° for this spur are often associated with a Warburg impedance (*36*) which corresponds to the effect of a diffusive boundary condition at the Pt electrode which is blocking to ionic species. More data would be required to confirm this effect (*7*). Spurs have only been observed in our studies when ionic diffusive species are present.

For the mixed conductor (b) the bulk semicircle is typically less well defined and tilted at a greater angle (here, $\alpha = 19°$) to the real axis. Evidence of a spur is shown, but it only becomes apparent at higher temperatures in comparison to type (a). For materials containing essentially electronic charges (e.g., Ti_4O_7, Fe_3O_4) no spurs were observed and the semicircles are inclined at high angles between 20° and 30° to the real axis (c). A perfect semicircle with zero angle of tilt is unrealistic and corresponds to a parallel combination of an ideal capacitor and a conductor; it is never observed in practice (*37*). More detailed AC studies of three electrically different types of catalyst will now be discussed. All three have been successfully used as catalysts to convert heavy oils to useful chemical feedstocks in a reactor heated by RF power (*10*).

Composite Containing a Fast-Ion Conductor

For a composite containing alumina, high-alumina cement, and the fast-ion conductor $K_{0.5}Mg_{0.8}Ti_{0.2}O_2$, the variation of the com-

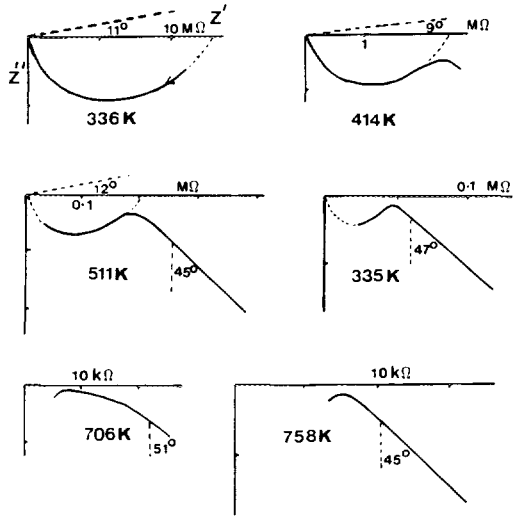

FIG. 3. Effect of temperature on complex impedance for a composite containing 35 wt% K–Mg–Ti–O.

plex impedance data with temperature is shown in Fig. 3. Up to 400 K, well defined semicircles have angles of tilt (α) of 9° ± 3°. Above 400 K a spur becomes attached until it becomes dominant at 1000 K. It is inclined at 48° ± 3° (β) to the Z'' axis at all temperatures. The critical frequencies f_A and f_B (defined in Fig. 2a) vary with temperature as shown in Fig. 4. The different effects of temperature indicate that different processes are responsible for behaviour in the "bulk" region and at f_A where different mechanisms overlap. Further measurements showed that f_A can be essentially attributed to processes occurring in the spur region. Here (100 Hz to f_a) the thermal effects will be associated with the activated diffusion of K^+ ions, and here both C_p and G/ω, in a single parallel circuit representation of the composite, are proportional to ω^{-n}, where n lies between 0.05 and 0.08. The observed behaviour is typical of materials showing an anomalous low frequency dispersion where thermally activated charge carriers dominate at low frequencies and high temperatures (*16, 17*). In the semicircular region (f_A to 2.5 MHz) relaxation losses from dipoles in both components may occur and the effective activation energy (at f_B) may be associated with a variety of processes.

According to the conventional interpretation of complex impedance spectra (e.g., Ref. (*14*)) the low-frequency spur is associated with electrode polarisation effects or the diffusion of "free" charge carriers and the higher frequency semicircle with dielectric losses in the bulk of the material. Angles α and β (Fig. 2a) are generally found to be independent of temperature as observed and an R–C network with parameters independent of frequency should be expected to fit the observed data reasonably well.

Since the angle α is small and complex admittance (Y'' vs Y') diagrams were found to be linear over the semicircle region (proof of a true semicircle (*32*)) a simple parallel R–C network could be fitted to the data above frequency f_A. For a perfect semicircle the relaxation frequency associated with this region is given by $(2\pi RC)^{-1}$ and at this point the loss tangent, tan δ, is unity. For this material f_B was found to be close to this value as expected. At frequency f_A in the region where two overlapping loss processes occur the loss tangent is at a peak.

The "bulk" conductance ($=R_b^{-1}$, where R_b is obtained by extrapolating the semicircle to the Z' axis as in Fig. 2a) shows well

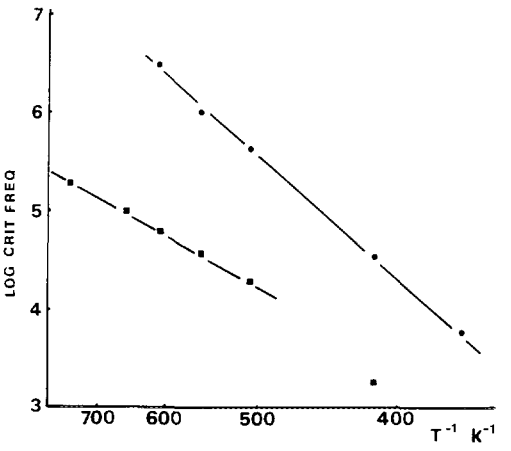

FIG. 4. Effect of temperature on critical frequencies for composite containing K–Mg–Ti–O at points f_A (■) and f_B (●).

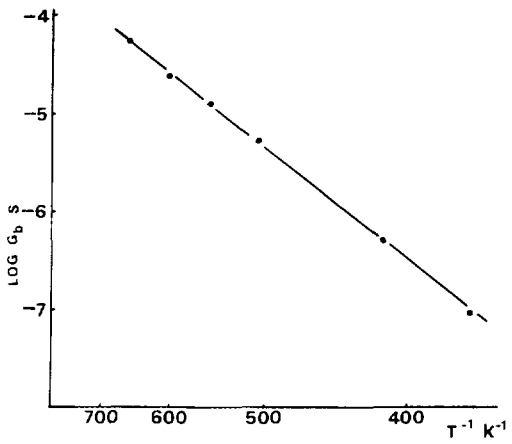

FIG. 5. Activated bulk conductance for composite containing K–Mg–Ti–O.

defined activated behaviour with an activation energy of 0.45 eV close to that determined for point f_B (Fig. 5). Figure 6 shows dielectric dispersion curves for a sample of similar composition (*38*) over the lower frequency range 0.01 Hz to 10 kHz. The low-frequency power law behaviour is clearly seen to be obeyed down to 0.01 Hz, with $G/\omega \propto \omega^{-1}$. Thus for this composite at low frequencies/high temperatures the conductivity was independent of frequency. The dielectric dispersion curves were normalisable over the temperature range 570 to 763 K. Such characteristic "universal" behaviour was also shown for a single component sample of a potassium magnesium titanate of hollandite structure (*16*) with $\sigma \propto \omega^{0.09}$. Thus, for this composite, the dielectric behaviour is dominated by the properties of the fast-ion conductor.

Composite Containing a Mixed Conductor

The complex impedance diagrams for a composite containing $K_{0.5}WO_3$ after preheating in air for 1 hr at 1000 K is shown in Fig. 7. The low-frequency spur appears at higher temperatures than those observed for the previous example; the bulk semicircle is less clearly defined and has a larger angle α of about 20° at all temperatures. At interme-

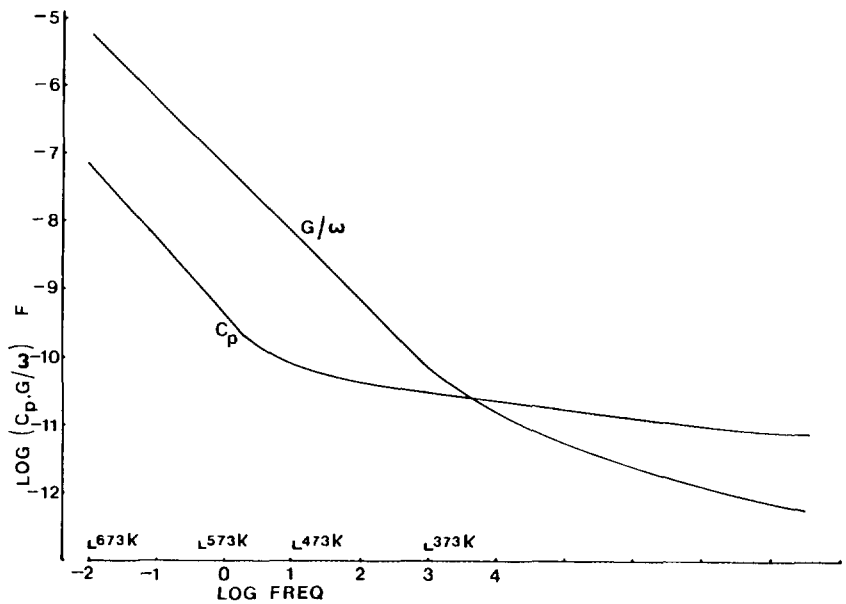

FIG. 6. Normalised dielectric frequency response for composite containing K–Mg–Ti–O. The scales are correct at 673 K and the curve shifts for other temperatures are given by the temperature-labelled datum points shown.

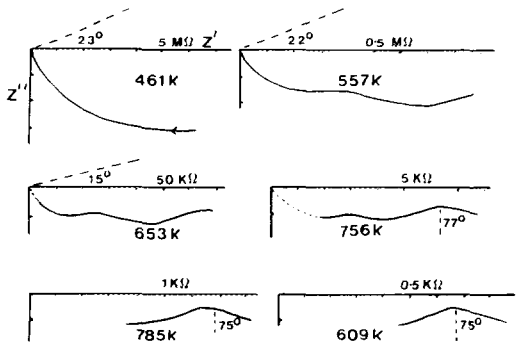

FIG. 7. Effect of temperature on complex impedance for a composite containing $K_{0.5}WO_3$.

diate frequencies an arc of a second semicircle is observed between 470 and 733 K. The appearance of a spur is to be expected, since the mixed conductor $K_{0.5}WO_3$, contains both electronic and ionic K^+ charge carriers (*4*). For a wide variety of supports all composites showed the angle of the spur to be independent of temperature. The critical frequencies for all parts of the impedance plots (from Fig. 7) shown in the schematic in Fig. 8a were found to have similar activation energies of 1 ± 0.1 eV (*7*). These frequencies may be correlated with those on the dielectric dispersion curves shown in Fig. 8b. At frequency f_A the log C_p vs log f relationship starts to deviate from linearity. The "bulk" region corresponds to frequencies $f > f_A$ where C_p and G/ω decrease more slowly with increasing frequency. For materials showing an intermediate frequency effect some distortion in the $C_p(f)$ characteristic is shown. At point f_C, tan δ exhibits a superimposed peak, (Fig. 8c). At f_D the frequency is close to that at which tan δ is unity.

Effect of atmosphere. The presence in the impedance plots of an arc at intermediate frequencies was only observed for some samples which has been preoxidised for 1 hr in air. This arc rapidly disappeared on adsorption of H_2 and is likely to be associated with dipole formation at the exposed surfaces of the porous material. At temperatures near 1000 K oxygen will partially dissociate and ionise. Some of the O^{2-} ions will be incorporated into surface O^{2-} vacancy sites, and must be paired with positive charges in the material. The subsequent surface dipoles will be subject to relaxation processes in an AC field. If there is interaction between neighbouring dipoles the relaxation will be non-Debye in nature and the resultant effect on the Z plots will be the superimposed arc shown. Since the frequencies associated with the two higher frequency regions are less than 2 decades apart, the semicircles overlap and are not well resolved; thus there is a spread of frequencies around f_C over which mixed phenomena occur. The middle arc was found to be highly

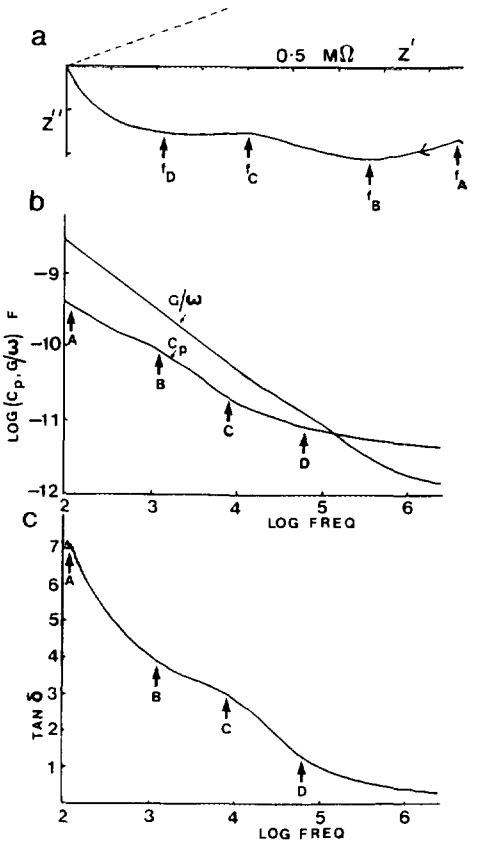

FIG. 8. Critical frequencies for a composite containing $K_{0.5}WO_3$ at 560 K (a) shown on dielectric–frequency curves (b) and on loss tangent-frequency characteristics (c).

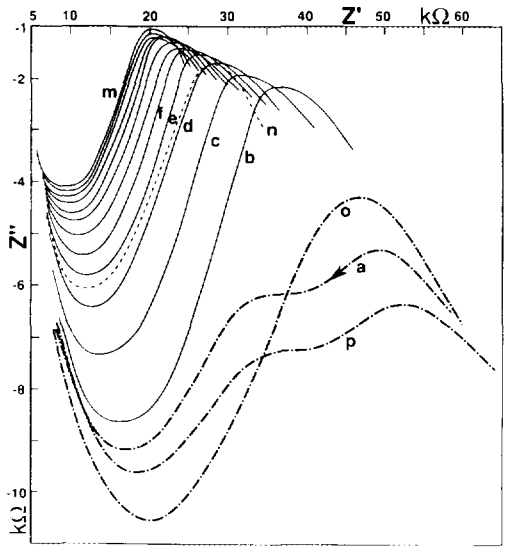

FIG. 9. Effect of oxidation and reduction on complex impedance for a composite containing $K_{0.5}WO_3$ at 747 K. Z'' scale exaggerated. (a) Initial oxidised state, (b)–(m) effect of hydrogen at 5-min intervals, (n) effect of CO_2 for 1 hr, (o) effect of air for 1 hr, and (p) effect of air for 1 hr at 950 K.

susceptible to gaseous atmosphere, as summarised in Fig. 9. After an hour's reduction in H_2, introduction of CO_2 had a slow oxidising effect at 750 K.

Air caused a more rapid response, but the intermediate arc could only be restored after preheating the sample in air for 1 hr at 950 K (7). It has consequently become associated with a rapid chemisorption effect. The critical frequencies associated with the different portions of the complex impedance curves showed activation energies of about 1.1 and 0.9 eV for the surface and bulk properties, respectively. On extrapolation of the spurs back to the Z' axis, an activation energy of about 0.82 eV was found to be associated with the spur region. Thus different processes must be responsible for the relatively free movement of charges at the lowest frequencies, the movement of surface charges (oxygen anions) at the intermediate frequencies and displacement of bound charges in the bulk of the solid at high frequencies. The behaviour is similar to the effect of atmosphere on lithium silicate glass (*39*).

At high temperatures H_2 will dissociate and ionise and the resulting protons and electrons will be able to rapidly diffuse throughout the material. The protons will combine with surface O^{2-} ions as OH^- groups or leave the surface as H_2O. Hence on adsorption of H_2 the observed electrical surface effects disappear. The combination of protons with internal more tightly bound oxygen anions will be more difficult and hence take longer. The conductivity will gradually increase as the concentration of bulk O^{2-} vacancies increases, with more sites becoming available for the remaining ions to move into. The proportion of both bulk and surface dipoles will also increase; hence the effective capacitance of the sample increases with time, whilst the resistance decreases. After heating in air, more loosely bound oxygen ions will be reintroduced, but due to the high activation energy required for the dissociation of O_2, high temperatures of the order of 1000 K are required for the surface effects to reappear.

The effects of atmosphere on the more conventional characteristics of conductance and parallel capacitance showed effects to be greatest at the lowest frequency with changes in G up to 124%. At low frequencies C_p increased to the same extent and is thus likely to be associated with the same phenomenon. However, at higher frequencies, atmosphere has less effect on C_p than on G. At 1 MHz, G increased by 86% after reduction, and C_p by 58% at 750 K. At 1 MHz impedance arises from lattice effects only, at 10 kHz surface dipole effects will occur, whilst at 100 Hz additional resistance will result from transport of more mobile charges.

Proportion of the conducting component. Due to the increasing proportion of the mobile charges the spur became increasingly dominant as the amount of the $K_{0.5}WO_3$ was increased from 10 to 50 wt%. The angle of the spur (β) was found to be slightly dependent on the proportion, but more dependent

TABLE 1

Critical Angles and Activation Energies for Composites with Variable wt% $K_{0.5}WO_3$

% $K_{0.5}WO_3$	Low-frequency spur		High-frequency semicircle	
	$\beta°$	E_A(eV)	$\alpha°$	E_A(eV)
10	72	0.91	18	1.1
30	72	0.87	20	0.87
50	65	0.79	22	0.84

on the nature of the support (type and proportion of cement and grade of alumina, etc.) (*7*). The activation energy associated with this low-frequency loss process was also found to be dependent on the nature of the support and to decrease as the amount of the conducting component was increased, as shown in Table 1. The low-frequency region must thus be related to the type of physical obstruction which the insulating grains offer to the mobile charges emanating from the conducting component.

In the bulk region the angle of tilt (α) was independent of temperature and (unlike β) also independent of the nature of the support but slightly dependent on the amount, with $\alpha = \pm 2°$. For each composite, the "bulk" conductance showed well defined activation energies (Fig. 10 and Table 1). Hence the physical phenomenon responsible for the tilt must depend essentially on the nature of the conducting component. For an ionically conducting zeolitic material α was found to depend on the density or porosity with α increasing as the density increased (*40*). It was not possible to tell whether the tilt arose from the bulk property or a grain boundary phase. As the amount of $K_{0.5}WO_3$ is increased the porosity of the composite is likely to decrease slightly (*1*) but α was found to increase somewhat, contrary to the zeolitic system. Thus the effect of porosity on the AC properties of the catalytic composites has yet to be determined and understood. Between 550 and 950 K the conductance associated with the bulk region increases rapidly with increasing proportion of the conductor, such that on average, at 750 K, $G_b \propto \exp(0.11)$ where x is the wt% (Fig. 11). The dielectric dispersion curves for each particular composite were normalisable, as shown, for example, in Fig. 12.

Supported Ni/SiO_2–Al_2O_3 Catalyst

Due to the high impedance of large supported Ni pellets as used in commercial applications, it was only possible to obtain reasonable impedance diagrams above 750 K. Typical curves for a sample with Pt contacts are shown in Fig. 13. The catalyst was in the reduced state having been previously reduced in a dilute stream of H_2 in Ar for 24 hr at 770 K. It was maintained in a reducing atmosphere (with flow rates of 25 and 100

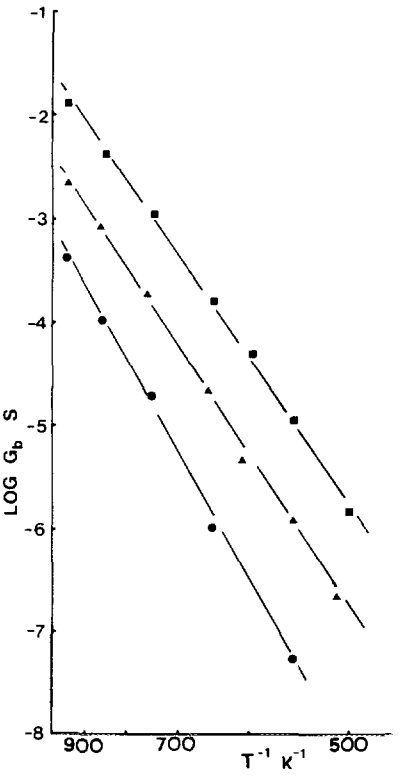

FIG. 10. Effect of the amount of the conducting component on the bulk conductance for (●) 10, (▲) 30, and (■) 50 wt% $K_{0.5}WO_3$.

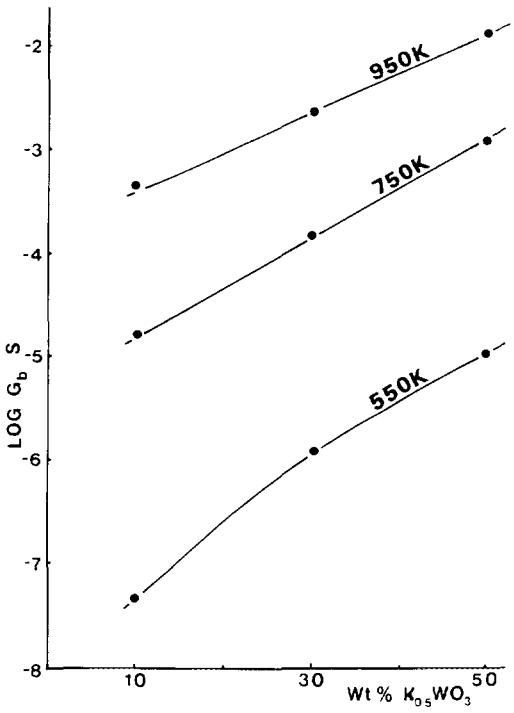

FIG. 11. Effect of the amount of $K_{0.5}WO_3$ on the bulk conductance at 550, 750, and 950 K.

ml/min of H_2 and Ar) throughout the electrical measurements. Lack of evidence of a well defined spur, even at the highest temperatures, indicates that there is negligible transport of ions in this material. Transport of electrons arising from the Ni particles is likely to occur via a substrate-assisted hopping mechanism (*41*). The impedance plots are shallow semicircles tilted to the real axis at about 20°. The activation energy associated with the bulk conductance in this region was about 0.89 eV. Experiments on another sample with Au rather than Pt electrodes showed almost identical behaviour, apart from generally higher impedances (as has been previously observed when Au contacts have been used). Pt can cause an enhancement in the conductivity due to its promotion of the dissociation of H_2 and consequent ionisation and release of electrons into the solid (*5*). It can be concluded that the nature of the electrode, as would be expected, has no significant effect on the bulk behaviour of this catalyst. Samples with a much higher area/depth ratio would be required for studies at lower temperatures.

DISCUSSION

Previous work on the electrical properties of porous catalyst composites has been found to correlate well with the Jonscher–Hill models for the dielectric behaviour of solids (*3*, *4*, *8*). When these materials contain a significant proportion of thermally activated "free" charge carriers a well defined power law for conductivity with $\sigma \propto \omega^n$ where $0 \leq n \leq 0.08$ coupled with high activation energies of the order of 1eV is observed at low frequencies/high temperatures. However, at high frequencies/low temperatures the charges are relatively immobile and behaviour is that of a "bound" or dipolar response. Here n may increase to values of about 0.8 and activation energies may approach zero. The dispersion curves have the same shape at all temperatures and may be superimposed ("normalised") by displacement of the frequency axes (as shown, for example, in Figs. 6 and 12). Thus temperature determines the frequency ranges over which the particular behaviour is prevalent.

At the high frequency end of the spectrum (up to 10 MHz) the dielectric properties are governed by relaxation losses and arise from impurity and structural defects in the lattice. Thus the low-power-law region (spur region on impedance graphs) is largely governed by the conducting component whilst the high-power-law region (bulk semicircle region on Z^* plots) may contain contributions from both the conducting and insulating components acting in parallel.

The technique of impedance spectroscopy has been largely developed and applied to the study of solid fast-ion conducting electrolytes for use in fuel cells, batteries, and sensors. The present results show that useful information can be gained by using this method of analysis for the more com-

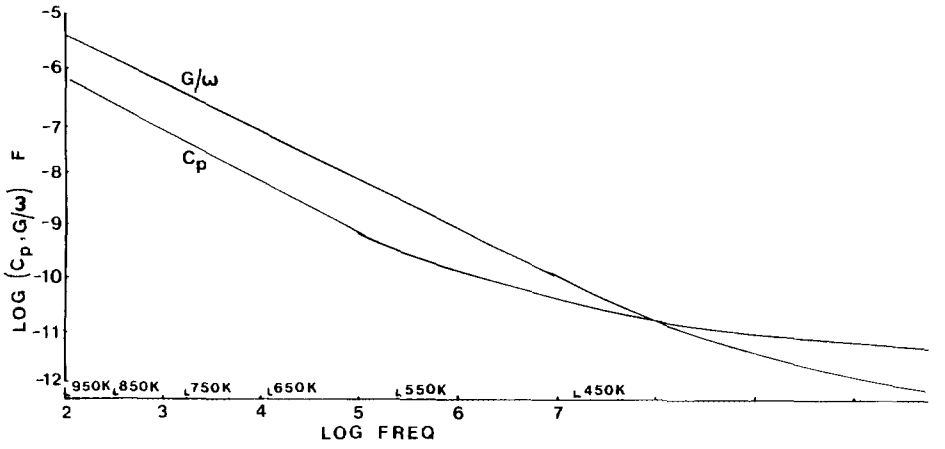

FIG. 12. Normalised dielectric–frequency response for a composite containing 35 wt% $K_{0.5}WO_3$. The frequency scale is correct at 950 K and is displaced as shown at lower temperatures.

plex multicomponent materials used in catalysis. The spectra cannot be fitted by the relatively simple circuits proposed for electrolytes, but the studies have shown that their shape can be revealing. The appearance of a spur indicates the presence of thermally activated mobile ions, whilst the presence of an arc at intermediate frequencies can be identified with rapid (and reversible) chemisorption processes. The high-frequency semicircle is associated with the bulk behaviour which may exhibit substantial changes if solid-state reactions occur or a slow oxidation or reduction of the material takes place in oxidising or reducing atmospheres. For materials containing mixed electronic and ionic conductivity, less well defined semicircles with larger angles of tilt are seen. Thus the shape of the complex impedance plane diagrams may initially reveal the nature of the dominant conducting species and the stability of the composite under reaction conditions.

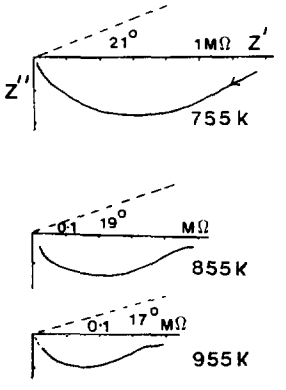

FIG. 13. Effect of temperature on complex impedance for a reduced supported Ni catalyst.

Jonscher has maintained that most solid dielectrics cannot be simulated by combinations of frequency-independent resistors and capacitors and that the perfect untilted semicircle is unrealistic (*32*, *36*, *37*). His alternative explanation for the observed tilted semicircles and spurs is consistent with the "universal" non-Debye behaviour which has been shown for a very wide range of materials (see also the introductory section on equivalent circuits). The angles α and β can then be related to the values of the index n relevant to the range of frequency concerned.

Low-Frequency/High-Temperature Region

No spurs were evident for composites containing purely electronic conductors such as semimetallic Ti_4O_7 or the low band-gap semiconductor Fe_3O_4. Hence diffusion of ions is associated with spurs and as pointed out by Jonscher (*32*) it is a barrier

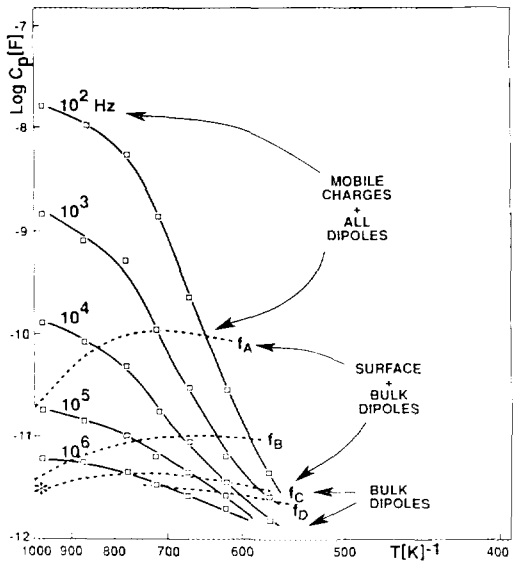

FIG. 14. Zones of dominant loss mechanisms on capacitance–frequency–temperature characteristics for a composite containing $K_{0.5}WO_3$. Asterisk indicates the position of reactor operation at 1000 K, 20 MHz.

effect, but whether it arises from electrodes or at internal barriers due to grain boundaries cannot be ascertained from AC data alone. The 45° spur shown in Fig. 3 could well be associated with a diffusive effect of K^+ ions and blocking at the electrode but it is not necessarily due to a Warburg impedance (*7*).

Since the measurements were restricted to the relatively high value of 100 Hz at the low-frequency end of the scale it is difficult to correlate the observations with theory to a quantitative extent. However, qualitatively the data are in good agreement with predictions. The model predicts that at high temperatures $\tan \delta = \cot (n\pi/2)$. For the range of composites examined, measurements of n at 1 kHz and 750 K showed agreement with this relationship to within 10%. The index n generally decreased as obstructions to diffusion of free charges were reduced by sintering (*8*) or by choice of the support material. Reduction in n is also accompanied by a reduction in the activation energy as the movement of charges becomes less restricted and influenced by the support.

The angle β and activation energy were found to depend on the proportion of the conducting component (Table 1) and depended significantly on the nature of the support. This is to be expected, since the motion of free charges will be partly affected by the size and shape of the adjacent grains.

High-Frequency/Low-Temperature Region

The angle of tilt of the semicircle was found to depend significantly on the type of conducting component; it increased from about 9° for a fast ion conductor to about 28° for a purely electronic additive. For the mixed conductor it was about 20° regardless of the nature of the support. Quantitative comparisons cannot be made accurately since at high frequencies n did not reach a constant value. In general, the higher is α the lower is n, with $\alpha = 90(1 - n)$. Hence for $\alpha = 20°$, n is expected to be about 0.78. Maximum values for various samples were about 0.8, which is close to the predicted value. As the proportion of tungsten bronze was increased from 10 to 50 wt%, the value of n, measured in each case at 450 K between 0.5 and 1 MHz, decreased from 0.82 to 0.73; the angle α increased from 18° to 22°. The values are within 11% of those predicted, providing further evidence that the "universal" model is applicable to these composite materials.

Only for materials containing fast ion conductors could be a reasonable R–C circuit be fitted to the data. A parallel R–C unit fits the high-frequency semicircle region, whilst in the spur region at lower frequencies the data are better fitted by an R–C series unit, but such that the components vary slightly with frequency.

Surface Effects

The dielectric model is however unable to differentiate between bulk and grain boundary or surface effects. It is here that the technique of impedance spectroscopy (with

its interpretations of interconnecting or overlapping semicircles in terms of separate loss processes) becomes particularly helpful. The appearance or otherwise of an arc at intermediate frequencies on the Z^* diagrams was found to be closely associated with rapid chemisorption processes.

Although these effects can be revealed by changes in G and C_p the separate effects on the bulk or surfaces of the material can only be shown up by impedance spectroscopy. Admittance plots, dielectric dispersion curves, or complex electric modulus plots were also examined, but did not give any further useful information.

The impedance data for composites cannot be accurately represented by a series of simple R–C networks. The principle use of the technique is in the determination of geometry-independent parameters such as angles of tilt, critical frequencies, and their associated activation energies. The critical frequencies at which changes occur on the Z^* diagrams can be used to define regions of dominant loss mechanisms on capacitance–temperature–frequency characteristics, as shown, for example, in Fig. 14 (*7*). For a reactor operating at 20 MHz, it is seen that the dielectric loss will arise from losses in both the bulk and surfaces of the material. The possibility of surface losses via movement of surface charges under operating conditions is likely to be linked to the good catalytic activity and selectivity observed at RF in the steam reforming of heavy oils (*10*). The separation of data into zones also reveals the temperature at which DC or low-frequency diffusion of ions ocurs. Such information would be useful for exploring the potential of using electromagnetic heating at lower frequencies. It must, however, be remembered that the energy absorbed is proportional to the AC conductivity, σ, so that if conditions are associated with high values of n, σ will decrease rapidly with decreasing frequency and the material may not be able to achieve the desired temperatures, without an increase in power consumption.

By examination of changes in Z^* plots under reaction conditions at high temperatures, or due to changes of atmosphere or changes of physical properties of the components, the stability of the AC conductivity and that of the catalyst itself may be evaluated. Thus impedance spectroscopy can help elucidate the catalytic behaviour in electromagnetic fields and assist in the design of composites for use in such fields. Here factors in the preparation, the overall dielectric loss, and the sensitivity to atmosphere and time are all important. The AC conductivity has been found to be relatively unaffected by changes in atmosphere at high temperatures at RF frequencies. Such effects are more significant at low frequencies. It is thus a useful method for studying chemisorption processes or monitoring a catalyst under *in-situ* conditions, which may lead to deactivation processes (such as sintering, fouling, poisoning or solid-state reactions between constituents).

The interpretation of more conventional dielectric dispersion curves and resultant $\sigma(\omega, T)$ relationships are useful for the prediction of behaviour based on the universal dielectric response. Further developments of more realistic physical models in terms of ion-hopping probabilities and possibly fractal behaviour of the materials (*42*, *43*) should assist in the future understanding of the AC properties of catalysts. This is important when considering the use of catalysts in RF or microwave fields and in the general understanding of catalytic activity.

As outlined in the Introduction, potential new catalytic materials are emerging from allied technologies which make use of conducting mixed oxides, and thus a deeper knowledge of the electrical behaviour of these materials could be both timely and fruitful.

CONCLUSIONS

AC electrical studies on insulator–conductor composites, for use as catalysts in an RF reactor, have shown that the two different methods of analysis of impedance

spectroscopy and complex permittivity frequency characterisation are not mutually exclusive, but that factors from each may be usefully combined.

At temperatures near ambient, complex plane impedance diagrams show whole or partial semicircular-like arcs inclined to the real axis; low angles of tilt below 10° have been observed when fast ion conductors are present and high angles up to 28° when charge carriers are largely electronic. As the temperature is increased to 1000 K a spur becomes attached at low frequencies when mobile ions are present. For mixed conductors (having significant electronic and ionic conductivities) a secondary arc may appear at intermediate frequencies. This arc is related to surface chemisorption processes and is clearly revealed on impedance spectroscopy curves but only weakly apparent in dielectric data.

The high frequency "semicircle" is associated with that portion of the dielectric dispersion curve (log ε' ($\propto C_p$), log ε'' ($\propto G/\omega$) vs log frequency) where both ε' and ε'' decrease slowly with frequency. Here, lattice dipole relaxation effects dominate those of more mobile charges. This region may be represented by a parallel combination of a frequency-independent conductance and a non-Debye dispersive frequency-dependent capacitance. At low frequencies, the addition of a spur is associated with the portion of the dielectric dispersion curve where both ε' and ε'' show a similar power law frequency dependence (typically $\propto \omega^{-0.95}$), a characteristic which is associated with thermally activated charge hopping and adequately described by the Jonscher theory of "universal" dielectric response. Here, the material is very "lossy" with $\tan\delta \gg 1$. The spur may be identified by a series element in the equivalent circuit, another capacitance of non-Debye nature having a high loss.

The critical frequencies at which changes occur in the impedance plots can be used to define the regions of different loss mechanisms (i.e., from mobile charges, surface and bulk dipole relaxation effects) on capacitance/temperature/frequency characteristics. Such characterisation can help to elucidate the catalytic behaviour under working conditions in electromagnetic fields and assist in the design of composites for use in such fields.

DC and AC electrical parameters are highly sensitive to changes arising from deactivation phenomena such as sintering, fouling and poisoning, phase changes, or solid-state reactions between components. Thus these techniques offer relatively simple and inexpensive ways of studying processes under realistic conditions.

Advances in allied areas (such as corrosion, sensors, specialist ceramics, electrodes, and electrolytes for use in solid fuel cells) take into consideration a wide range of chemical, physical and structural properties. Thus recent knowledge in these rapidly advancing fields could aid the design of catalysts. In particular, recent technological progress has highlighted the potential use of mixed oxide materials as components in catalysts for oxidation reactions.

ACKNOWLEDGMENTS

The authors are grateful to the SERC for the purchase of the analytical equipment, and to S. Miri and T. Mirza for the preparation of samples. Particularly helpful comments on this paper were provided by Professor R. M. Hill.

REFERENCES

1. Ovenston, A., Miri, S., and Walls, J. R., *in* "Advanced Ceramics in Chemical Processing Engineering" (B. C. H. Steele and D. P. Thompson, Eds.), Ser. Brit. Ceram. Proc., Vol. 43, p. 57. Inst. Ceram., London, 1989.
2. Ovenston, A., and Walls, J. R., *Trans. I. Chem. Eng.* **68,** 530 (1990).
3. Ramdeen, T., Dissado, L. A., and Hill, R. M., *J. Chem. Soc. Faraday Trans. I* **80,** 325 (1984).
4. Ovenston, A., Walls, J. R., Miri, S., and Ramdeen, T., *J. Phys. D* **21,** 1773 (1988).
5. Ovenston, A., and Walls, J. R., *Sens. Actuators* **12,** 159 (1987).
6. Herrmann, J-M., and Pichat, P., *J. Catal.* **78,** 425 (1982).
7. Ovenston, A., and Walls, J. R., *Solid State Ionics* **53–56,** 825 (1992).

8. Ovenston, A., and Walls, J. R., *Solid State Ionics* **44,** 251 (1991).
9. Ovenston, A., and Walls, J. R., *J. Phys. D: Appl. Phys.* **17,** L101 (1984).
10. Mirza, M. T., Walls, J. R., and Jayaweera, S. A. A., *Thermochim. Acta* **152,** 203 (1989).
11. Atkinson, A., and Monty, C., *in* "Surfaces and Interfaces in Ceramic Materials" (L. C. Dufour, C. Monty, and G. Petot-Ervas, Eds.) p. 273. Kluwer, Dordrecht, 1989.
12. Atkinson, A., *J. Chem. Soc. Faraday Trans.* **86,** 1307 (1990).
13. Archer, W. I., and Armstrong, R. D., *Chem. Soc. Spec. Per. Rep., Electrochem.* **7,** 157 (1980).
14. Kilner, J. A., *Mater. Sci. Forum* **7,** 205 (1986).
15. Jonscher, A. K., *Nature* **267,** 673 (1977).
16. Jonscher, A. K., *Philos. Mag. B* **38,** 587 (1978).
17. Hill, R. M., and Jonscher, A. K., *Contemp. Phys.* **24,** 75 (1983).
18. Sleight, A. W., *Science* **208,** 895 (1980).
19. Gellings, P. J., and Bouwmeester, H. J. M., *Catal. Today* **12,** 1 (1992).
20. Pritchard, J., *Nature* **343,** 592 (1990).
21. Vayenas, C. G., Bebelis, S., and Ladas, S., *Nature* **343,** 625 (1990).
22. Thomas, J. M., *Solid State Ionics* **32–33,** 869 (1989).
23. Tejuca, L. G., Fierro, J. L. G., and Tascon, J. M. D., *Adv. Catal.* **36,** 237 (1989).
24. Thomas, J. M., *Adv. Mater.* **8,** 255 (1989).
25. Carberry, J. J., Rajadurai, S., Alcock, C. B., and Li, B., *Catal. Lett.* **4,** 43 (1990).
26. Muragaraj, P., and Maier, J., *Solid State Ionics* **32–33,** 993 (1989).
27. Haralambous, K. J., Loizos, Z., and Spyrellis, N., *Mater. Lett.* **11,** 133 (1991).
28. Von Hippel, A. R., "Dielectric Materials and Applications." MIT Press, Cambridge Mass., 1954.
29. Ovenston, A. and Walls, J. R., *J. Chem. Soc. Faraday Trans. 1* **79,** 1073 (1983).
30. Ovenston, A., Ph.D. thesis, Teesside Polytechnic, UK, 1980.
31. Coelho, R., "Physics of Dielectrics." Elsevier, Amsterdam, 1979.
32. Jonscher, A. K., *J. Mater. Sci.* **13,** 553 (1978).
33. MacDonald, J. R., "Impedance Spectroscopy." Wiley, Chichester, 1987.
34. Reddy, S. N., Chary, A. S., Shahi, K., and Chiranjivi, R., *J. Mater. Sci: Mater. Electron.* **1,** 153 (1990).
35. Ovenston, A., *Solid State Ionics,* **58,** 221 (1992).
36. Jonscher, A. K., *Phys. Status Solidi (a)* **32,** 665 (1975).
37. Jonscher, A. K., *J. Mater. Sci.* **24,** 372 (1989).
38. Ramdeen, T., personal communication.
39. Reid, W. B., and West, A. R., *Solid State Ionics* **28–30,** 681 (1988).
40. Skou, E. M., and Jacobsen, T., *Appl. Phys. A* **49,** 117 (1989).
41. Hill, R. M., *Nature* **204,** 35 (1964).
42. Funke, K., *Mater. Res. Soc. Symp. Proc.* **210,** 97 (1991).
43. Dissado, L., and Hill, R. M., *Phys. Rev. B* **37,** 3434 (1988).